

Article

# Investigation of Itaconic Acid Separation by Operating a Commercialized Electrodialysis Unit with Bipolar Membranes

Tamás Rózsenberszki \*, Péter Komáromy, Enikő Kőrösi, Péter Bakonyi, Nándor Nemestóthy and Katalin Bélafi-Bakó

Research Group on Bioengineering, Membrane Technology and Energetics, Faculty of Engineering, University of Pannonia, 10. Egyetem str., 8200 Veszprém, Hungary; komaromy.peter@mk.uni-pannon.hu (P.K.); korosi.eniko95@gmail.com (E.K.); bakonyip@almos.uni-pannon.hu (P.B.); nemesn@almos.uni-pannon.hu (N.N.); bako@almos.uni-pannon.hu (K.B.-B.)

\* Correspondence: rozsenberszki.tamas@uni-pannon.hu; Tel.: +36-(88)-624-385

Received: 10 July 2020; Accepted: 17 August 2020; Published: 24 August 2020



**Abstract:** Nowadays, the merging of membrane and fermentation technologies is receiving significant attention such as in the case of itaconic acid (IA) production, which is considered as a value-added chemical. Its biotechnological production is already industrially established; however, the improvements of its fermentative and recovery steps remain topics of significant interest due to sustainable development trends. With an adequate downstream process, the total price of IA production can be reduced. For the task of IA recovery, a contemporary electro-membrane separation processes, electrodialysis with bipolar membranes (EDBM), was proposed and employed in this work. In the experiments, the laboratory-scale, commercialized EDBM unit (P EDR-Z/4x) was operated to separate IA from various model solutions comprised of IA (5–33 g/L), glucose (varied in 15–33 g/L as a residual substrate during IA fermentation) and malic acid (varied in 0–1 g/L as a realistic by-product of IA fermentation) under different initial pH (2–5) and applied potential conditions (10–30 V). Unambiguously negative effects related to the glucose and malic acid as impurities were found neither on the IA recovery ratio nor on the current efficiency, falling into the ranges of 90–97% and 74.3–98.5%, respectively. The highest IA recovery ratios of 97% and 98.5% of current efficiency were obtained with the model fermentation solution containing 33 g/L IA, 33 g/L glucose at 20 V and an initial pH of 5. However, the selective separation of IA needs further investigations with a real fermentation broth, and the findings of this research may contribute to further studies in this field.

**Keywords:** bipolar membrane; electrodialysis; itaconic acid; by-product; integrated system

## 1. Introduction

Itaconic acid (IA) or 2-methylidenebutanedioic acid is considered as a widely applicable, bio-based compound. In fact, this di-carbonic unsaturated acid can be utilized as a chemical building block because of its beneficial properties [1]. Due to the conjugated double bond of the methylene group, it can be polymerized by addition and condensation [2], and it has acquired the market position of an important platform chemical [3]. The growth of the IA market could be facilitated via approaches that allow for a reduction in the relatively high production and recovery costs of the acid [1]. Although IA fermentation has a more or less 100-year-old history, a recent and significant interest in the topic can be observed approximately from 2012 (based on Scopus database), showing that relevant methods are under intense research and development [4,5]. The interest in IA has two main directions: one is the traditional polymer industry with several applications such as plastics, adhesives elastomers,

coatings [6]. Besides IA can be utilized as bio-based green solvent or in hydrogel composites intended for biomedical applications such as ophthalmic, dental and drug delivery fields [6–8].

The widely applied genera for the biotechnological production of IA is *Aspergillus* [4,9,10], as well as some others, for instance *Ustilago* and *Pseudozyma* [11,12]. The most common substrate is glucose, which is metabolized into IA as detailed in the previous literature [13,14]. The fermentative IA production titer from sugar is able to reach more than 80 g/L [6]. However, along with the formation of IA from glucose, side-products such as malic acid (MA), alpha-ketoglutaric acid, fumaric acid, and some metal containing molecules (in much lower quantity) are commonly generated [15]. Moreover, at the end of the fermentation, residual glucose may be present in the broth [16]. Consequently, there can be a considerably complex, typically acidic mixture with a pH of around 3 from which IA has to be recovered [15,17].

The separation of organic acids, e.g., IA, seems to be manageable by membrane technology such as electrodialysis using bipolar membranes (EDBM), which can provide sufficient selectivity [18]. Several techniques were studied for the separation of IA, such as crystallization, precipitation, extraction, electrodialysis (ED), diafiltration, pertraction, and adsorption [18]. According to Magalhães et al., membrane separation and reactive extraction are promising options for the efficient separation following fermentation [18]. Recently, Varga et al. investigated the electrodialysis unit for the separation of IA [19]. It was found and confirmed that ED equipped with monopolar membranes can be applied successfully for the separation of IA from residual glucose as the main component (substrate) in the fermentation broth. The attention towards the separation of organic acids by EDBM has grown considerably in the last decade. According to Okabe et al. [6], the industrial production of IA is a multi-step (five step or more) batch process. Typical stages for the production of IA are as follows: fermentation, filtration, concentration, two series of crystallization processes and decolorization. Additional processes to enhance the purity of the product (IA) are solvent extraction, ion exchange, and further decolorization. The connection of the IA fermentation process with the EDBM separation technique can reduce the number of required purification steps and, hence, the design of such integrated systems could be seen as a way forward. In fact, the biologically catalyzed IA formation is determined by strict biochemical mechanisms and, thus, design of integrated systems can be suggested to take IA continuously away from the fermentation mixture. Moreover, continuous operation with the coupled fermentation–electrodialysis system can mitigate the inhibition (due to the accumulation of the product) by maintaining a sufficiently low IA concentration [20].

In this work, we investigated the emerging electro-membrane process, EDBM, to recover IA from various model fermentation mixtures containing IA and plausible impurities (glucose and MA, in agreement with the above). Apart from the effect of EDBM inlet composition and its pH, the impact of applied potential on the IA recovery ratio and current efficiency (CE) was tested experimentally using a commercialized electrodialysis apparatus. The experimental conditions were considered based on our previous, relevant work [21]. To our knowledge, this subject has not yet been specifically investigated, and the data generated and assessed in this paper show an added value that may enrich the literature.

## 2. Materials and Methods

### 2.1. Chemicals

The following chemicals were used during the EDBM experiments: itaconic acid (Acros Organics™; purity: >99%), Na<sub>2</sub>SO<sub>4</sub> (Sigma-Aldrich; purity: >99%), L(-) malic acid (Sigma-Aldrich; purity: 97%; optical purity: 99%) and glucose (Sigma-Aldrich; purity: >99.5%). The pH was adjusted by sodium hydroxide (pH = 5) and sulfuric acid (pH = 2 and pH = 3). Chemicals were analytical grade and purchased from Sigma-Aldrich.

## 2.2. Experimental Setup

The IA separation experiments were conducted on a laboratory-scale electro dialysis unit (P EDR-Z/4x), manufactured by the Czech company MemBrain®. The device was operated as an EDBM-Z/4x10-0.8 variant (Table 1) featuring 10 membrane triplets, where each triplet contained an arrangement of ion-conductive cation-, bipolar-, and anion-exchange membranes (RALEX®, MEGA corp., Czech Republic) (Table 2). Bipolar membranes are composed of both anion and cation layers.

**Table 1.** EDBM-Z/3x10-0.8 specification and operating limits.

Parameter	Value
Effective surface of the membrane module	1984 cm <sup>2</sup>
Effective surface of one membrane in the module	64 cm <sup>2</sup>
General size of membranes	56 × 206 mm
Effective size of membranes	40 × 160 mm
Number of the membrane cells	10 pieces
RALEX® anion exchange membrane AM(H)-PP	10 pieces
RALEX® cation exchange membrane CM(H)-PP	11 pieces
RALEX® bipolar membrane (PP)	10 pieces
Thickness of the spacer	0.8 mm
Electrode (anode, cathode), Ti/Pt	2 pieces
Size of ED module	135 × 90 × 250 mm
Weight of module with preservation solution	1.9 kg
Operating flow-rates	25–60 L/h
Min. and Max. temperature	10–35 °C
Operating voltage	3 V/triplet
Max. voltage/current	35 V/3 A

**Table 2.** Features of the RALEX® membranes.

Type of Membrane	Characteristics	
<b>Anion-exchange membrane</b> RALEX® AMH-PES	Permselectivity (0.5/0.1 M KCl)	>90%
	Resistance in 0.5 M NaCl, DC current	<7.5 Ωcm <sup>2</sup>
	Stability	Acid, base, thermal (max 50 °C)
	Thickness of swollen membrane	<0.75 mm
	Transport number (0.5/0.1 M KCl)	>0.95%
<b>Cation-exchange membrane</b> RALEX® CMH-PES	Permselectivity (0.5/0.1 M KCl)	>90%
	Resistance in 0.5 M NaCl, DC current	<8 Ωcm <sup>2</sup>
	Stability	Acid, base, thermal (max 50 °C)
	Thickness of swollen membrane	<0.70 mm
	Transport number (0.5/0.1 M KCl)	<0.95%

The EDBM setup was equipped with four-chambers, namely, diluate (D), electrolyte (E), acid (C<sub>acid</sub>), base (C<sub>base</sub>). To begin the measurements, 1 L of the actual (feed) model solution was loaded to tank D; C<sub>base</sub> and C<sub>acid</sub> (in which IA was collected during the separation) contained 1 L of DI water, while tank E was filled with 200 mL of 0.5 M Na<sub>2</sub>SO<sub>4</sub> solution. The following flow (recirculation) rates were maintained during operation: C<sub>base</sub>: 50 L/h; D: 50 L/h; C<sub>acid</sub>: 50 L/h; E: 60 L/h. The feed solutions were formulated as stated in Table 3, based on our previous experiences with IA production and separation [21,22]. The conductance of the solutions (in tanks D, C<sub>base</sub>, C<sub>acid</sub>) over time was measured by a Radelkis OK-102/1 conductivity meter connected to a Radelkis OK-9023 bell electrode using a cell constant of 0.7 cm<sup>-1</sup>. All the conductance data were acquired by a National Instruments USB-6009 14-Bit multifunction DAQ USB device and analyzed online using LabVIEW software. Current values were measured by a Metrix MTX3281B Handheld Digital Multimeter connected to SX-DMM v 2.3 software.

**Table 3.** The experimental plan executed in this work.

ID of the Experiment	IA Conc. (g/L)	Glucose Conc. (g/L)	MA Conc. (g/L)	Potential (V)	pH <sub>initial</sub>
A.	5	15	0	30	2
B.	33	33	0	20	5
C.	5	15	0.5	10	3
D.	10	25	0.75	10	3
E.	15	33	1.0	10	3

### 2.3. Analytical Methods

The concentrations of IA and MA were followed by a Young Lin Instrument Co., Ltd. high-performance liquid chromatography (HPLC) system (including a YL9109 vacuum degasser, a YL9110 quaternary pump and a YL9150 automatic sample dispenser) with a Hamilton PRP-X300 HPLC column 15 cm in length, 4.6 mm inner diameter, 5  $\mu$ m particle size (Hamilton Company, Berkeley, CA, USA) and a YL9120 UV/VIS detector. The 3,5-dinitrosalicylic acid (DNS) method [23] was used to analyze the reducing sugars—in our case, glucose (DR3900 Laboratory VIS Spectrophotometer, 575 nm wavelength).

### 2.4. Calculations

To evaluate the data from EDBM experiments carried out under the conditions tabulated in Table 3, the current efficiency ( $\eta_{\text{current}}$ ) was calculated in accordance with Equation (1):

$$\eta_{\text{current}} (\%) = 100 * Q_{\text{theoretical}} / Q_{\text{actual}} \quad (1)$$

where

$$Q_{\text{theoretical}} = E_m * b * F \quad (2)$$

$$Q_{\text{actual}} = \int Idt * N \quad (3)$$

In Equation (2),  $E_m$  is the total mass equivalent of IA, which is theoretically transferred (mol);  $b$  is 2 for fully dissociated IA; and  $F$  is the Faraday constant (96,500 C/mol). In Equation (3),  $N$  is the number of cell pairs (10 in this study),  $I$  is the measured current (A) and  $t$  is the operation time of the separation process [24]. The resistance of the segments (diluate,  $C_{\text{base}}$ ,  $C_{\text{acid}}$ ) was calculated by Ohm's law using the voltage data measured using the Ti wire between the segment pairs in the membrane module.

In the case of IA, the product recovery (PR) is the ratio between the concentration of IA (g/L) in the  $C_{\text{acid}}$  tank at the end of separation ( $C_{\text{acid}}^{\text{IA}}$ ) and the concentration of IA (g/L) in the diluate tank filled with the feed solution at the beginning of the separation (Diluate<sup>IA</sup>) presented in the Equation (4) [25].

$$\text{PR} = \frac{C_{\text{acid}}^{\text{IA}}}{\text{Diluate}^{\text{IA}}} * 100\% \quad (4)$$

## 3. Results and Discussion

As mentioned, EDBM technique provides an attractive solution to remove acid (IA in this case) in a system integrated with fermentation. Furthermore, the base generated in the EDBM process can be used for controlling the pH in the bioreactor. When applying the EDBM, there is a possibility to separate the acid with a relatively high concentration (which is beneficial for further purification steps), and at the same time keep its concentration low in the media in order to increase the productivity (by overcoming the feedback inhibition effect) [26].

The suspended solids and mycelium can be filtered from the broth before the separation; however, the dissolved substances, such as the substrate of fungus, can be not filtered. One of the most commonly used substrate during the IA fermentation process is glucose [13,14]. Thus, the test solutions contained

glucose to simulate the residual substrate. Previous experiments showed that IA separation from simple model solutions could be managed and reached a CE of over 91% with a similar system configuration and parameter settings (pH = 5, 20 V applied potential and 33 g/L IA model solutions) [21]. During a continuous operation, the presence of the substrate and, furthermore, the production of by-products such as succinic, malic acid, alpha-ketoglutaric acid, fumaric acid etc. are inevitable [27]. In the present study, further tests were carried out not just to optimize the IA separation but to additionally examine the impact of the fermentation by-product (MA).

### 3.1. Preliminary Tests without Applied Electrical Potential (Standbymode)

Firstly, a model solution with 33 g/L IA content was tested without an electrical field to analyze the non-electro-based effects from the perspective of IA separation. By the end of the experiment, from 33 g IA, less than 0.5 g was transported through the membranes, probably due to concentration diffusion. The final concentration of IA was 27 g/L. Without the force of potential difference (the DC supply was turned off), it was hypothesized that the rest of the IA may adsorb in the membrane module, particularly on the surface of membranes (membranes surface area: 1984 cm<sup>2</sup>). However, further experiments showed that the adsorption effect was negligible during the operation when it was under the driven force of potential difference.

The scheme of the EDBM system (used in this work) and the main mass transport mechanisms are presented in Figure 1, which will be considered for the discussion of the results in Section 3.4.

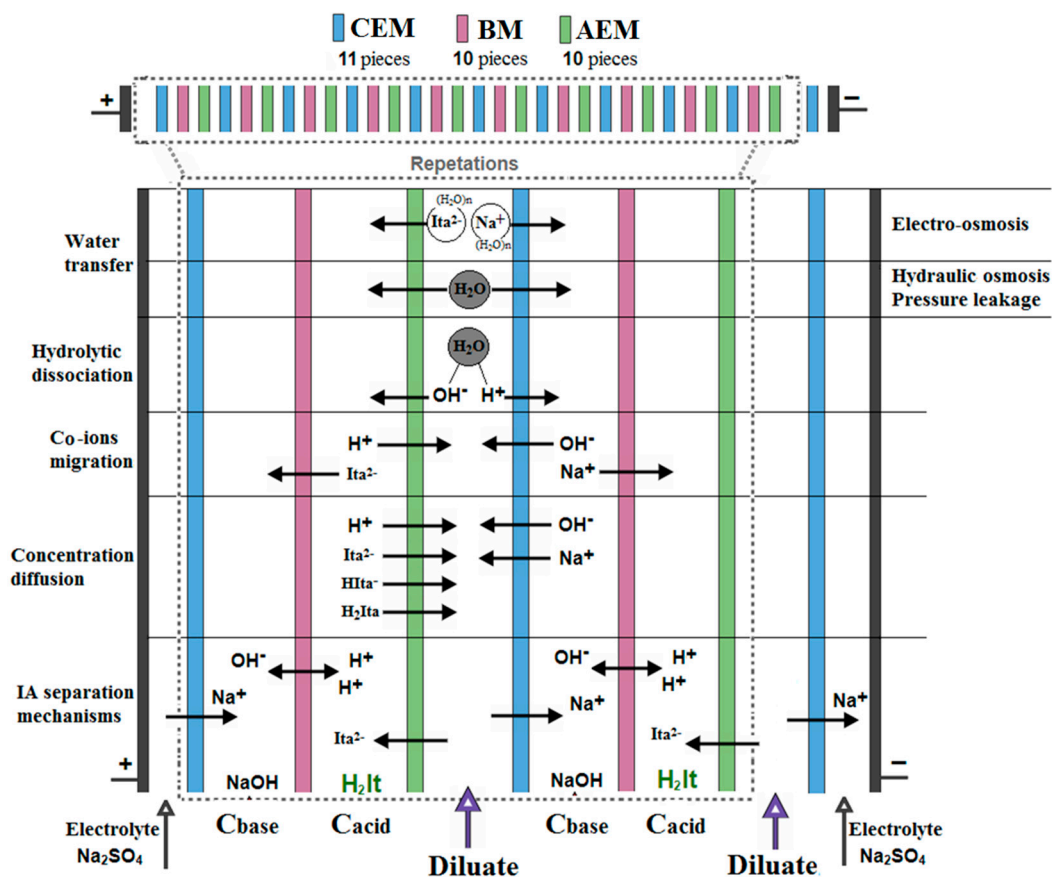


**Figure 1.** Schematic of the four mass transfer mechanisms which can cause a change in the concentration and/or volume during the separation by electrodialysis with bipolar membranes (EDBM) [28]. Illustration displays the itaconic acid (IA) separation mechanisms and schematic of the membrane module which was applied during the experiments described in the present work. CEM: cation-exchange membrane; BM: bipolar membrane; AEM: anion-exchange membrane.

### 3.2. Effects of Hydroxide and Hydrogen Ions on the Separation Parameters in EDBM

The experiments demonstrated in the following chapters were performed under the applied electrical field. On the one hand, as mentioned above, a typical pH of the IA fermentation is 3, however without strict pH control it can decrease due to the acidification [17]. On the other hand, assuming a continuous system the fermentation broth which is recycled and already treated by the EDBM can have a pH higher than 3. Thus, the tests in this work were conducted in the pH range 2 to 5. Present measurement was carried out on model solution containing 5 g IA/L with an initial pH of 2, mimicking a real fermentation broth. The separation of IA was carried out under 30 V of applied voltage. The diagram (a) in Figure 2 illustrates the conductance of segments  $C_{acid}$ ,  $C_{base}$ , diluate and the concentration of IA (dotted line) in the  $C_{acid}$ . As can be seen, the conductance of diluate continuously decreased during the operation due to the transport of the itaconate ions, which correlates well with the observed change in the IA concentration in  $C_{acid}$  based on the spectrophotometric (absorbance) data. In the course of the separation, the conductance of  $C_{base}$  and  $C_{acid}$  was increasing, and then decreased after approximately 45 min. The registered increase was a consequence of two main phenomena, namely, the migration of ions from the diluate side, and the influence of the  $OH^-$  and  $H^+$  ions exhibiting anomalously high mobilities in aqueous solutions [29]. The mentioned decreasing trend was caused by the reduced influence of hydroxide ( $OH^-$ ) and hydrogen ( $H^+$ ) ions generated by the bipolar membranes during the separation process. Similar phenomena were reported by Wang et al. [30].

The data regarding pH in  $C_{base}$  (triangled) and  $C_{acid}$  (dotted) are shown in diagram (b) of Figure 2. A slight decrease and increase in pH were noticed in the case of  $C_{base}$  and  $C_{acid}$ , respectively, from around 45 min, which supports the explanation of the phenomena linked to the drop in conductance. The results imply that the decline in conductance linked to  $C_{base}$  and  $C_{acid}$  was mainly associated with the smaller influence of  $OH^-$  and  $H^+$  ions (formed at the bipolar membranes) rather than with the migration of IA. Additionally, there is a strong correlation between the conductance of solutions in the segments (D,  $C_{base}$ ,  $C_{acid}$ ) and the current flow measured through the membrane stack. During the ED process, the diluate segment gradually decreased in terms of amount of ions and, thus, the resistance increased and the electric current decreased. Consequently, the phenomena (described above) are supported based on the electric current diagram (c) in Figure 2.

### 3.3. Influence of the Presence of Substrate

In these experiments, 20 V and 30 V potentials were applied, and the initial pH was adjusted to 2 and 5 (shown in Table 3, ID of experiments are A and B).

The results showed (as seen in Table 4) that the residual glucose in all cases could not pass through the membranes, while IA was able to separate with a high rate (PR: >90%). Sun et al. achieved similar PR (>97%) of citric acid using EDBM from fermented liquid containing sodium citrate of 3.3% [31]. In operation A. (shown in Table 3), under high potential of 30 V and a low initial pH of 2, IA appeared in the segment  $C_{base}$  (0.4 g/L) due to the co-ion migration through the bipolar membranes described in Figure 1. Due to the fact that there was no accomplished membrane with 100% permselectivity, transport of undesired ions through the membranes (co-ion migration) caused negative impacts on the process efficiency.

From the viewpoint of CE, the lower potential and higher concentration of IA were preferable, but further investigation is needed because there are a lot of parameters (flow rate, temperature, other ionic substances, etc.) which may have influenced to the columbic utilization. Figure 3 demonstrates the current curves, the resistance calculated of the segments and the conductance of circulated solutions (diluate,  $C_{base}$ ,  $C_{acid}$ ) during the separation process. The tendency of these data could indicate and characterize the ionic transport mechanisms. The maximum electric current reached 392 mA and 538 mA during experiment A and B, respectively.

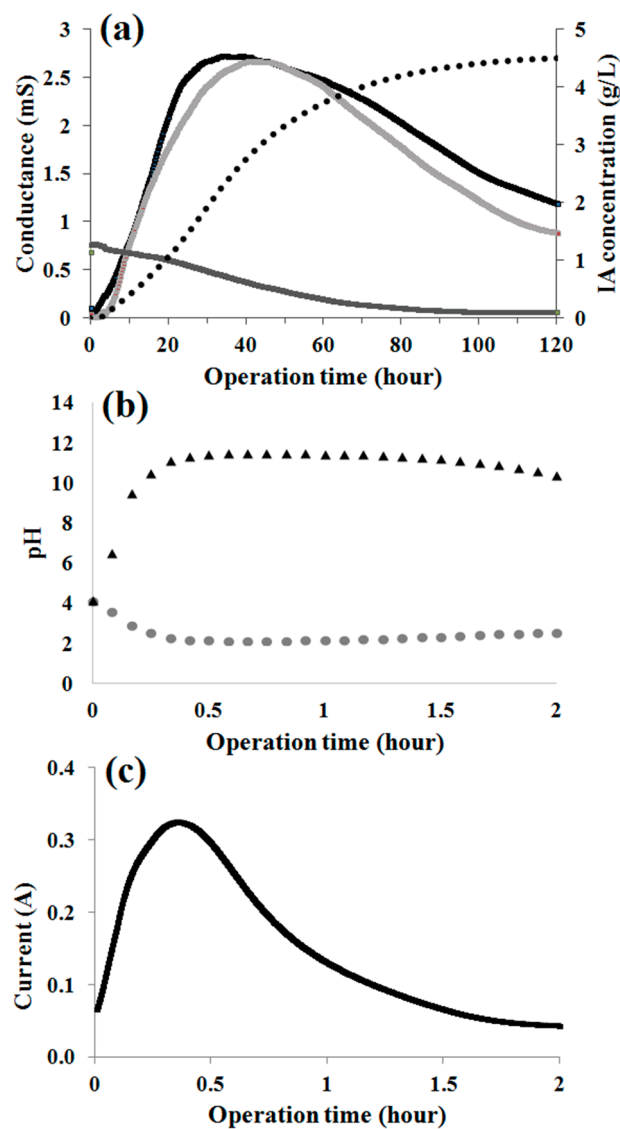


**Figure 2.** Effect of the ions generated by the water splitting by bipolar membranes in the EDBM system. During the test, diluate was fed with the solution containing 5 g/L IA, pH was adjusted to 2, and 30 V potential was applied. Legend of the diagram (a): C<sub>acid</sub>: black line; C<sub>base</sub>: light grey line; Diluate: grey line. Legend of the diagram (b): C<sub>base</sub>: triangled; C<sub>acid</sub>: dotted.

During the separation process, mobile ions were transferred, while water dissociation ( $\text{H}_2\text{O} \rightarrow \text{H}^+ + \text{OH}^-$ ) was induced by bipolar membranes (Figure 1), causing low resistance level of all the segments (Figure 3). Afterwards, when the transport of ions slowed down, the resistance level of the segments increased (C<sub>acid</sub>, diluate) or stagnated (C<sub>base</sub>) due to the lower availability of mobile ions. The resistance of C<sub>acid</sub> and diluate became significantly larger. In the latter case, this occurred due to the migration of ions to the adjacent segments. At a higher applied potential (30 V) in the experiment “A”, itaconate could be detected (0.5 g/L) in the C<sub>base</sub> segment (seen in Table 4) and probably could be found in the membrane phase, leading to higher internal potential and lower CE (74.3%) compared to experiment “B” (98.5%). This means that high potential could negatively affect the separation (under the conditions of this work). The phenomena described above can be supported by the results seen in the conductance curves in Figure 3 (dashed and grey line).

**Table 4.** Summary of the data measured during the IA separation experiments in accordance with Table 3.

Segment	ID: A.			ID: B.			ID: C.			ID: D.			ID: E.		
	Diluate	C <sub>base</sub>	C <sub>acid</sub>												
Initial volume (mL)		1000			1000			1000			1000			1000	
Final volume (mL)	980	1000	960	960	980	1000	850	960	1120	960	990	980	960	970	970
Initial conc. of glucose (g/L)	15	0	0	33	0	0	15	0	0	25	0	0	33	0	0
Final conc. of glucose (g/L)	15	<0.1	<0.1	32	<0.1	<0.1	15	<0.1	<0.1	25	<0.1	<0.1	32	<0.1	<0.1
Initial conc. of IA (g/L)	5	0	0	33	0	0	5	0	0	10	0	0	15	0	0
Final conc. of IA (g/L)	<0.1	0.5	4.5	<0.1	<0.1	32	<0.1	0.4	4.5	<0.1	1	9	<0.1	1	14
Initial conc. of MA (g/L)			No MA added				0.5	0	0	0.75	0	0	1.0	0	0
Final conc. of MA (g/L)			No MA added				<0.1	<0.2	<0.3	<0.2	<0.2	0.3	<0.3	<0.3	0.3
Operation time (hour)		1.5			4.0			5.0			8.0			9.0	
CE (%)		74.3			98.5			78.3			97.9			98.5	
Product recovery (%)		90			97			90			90			93	

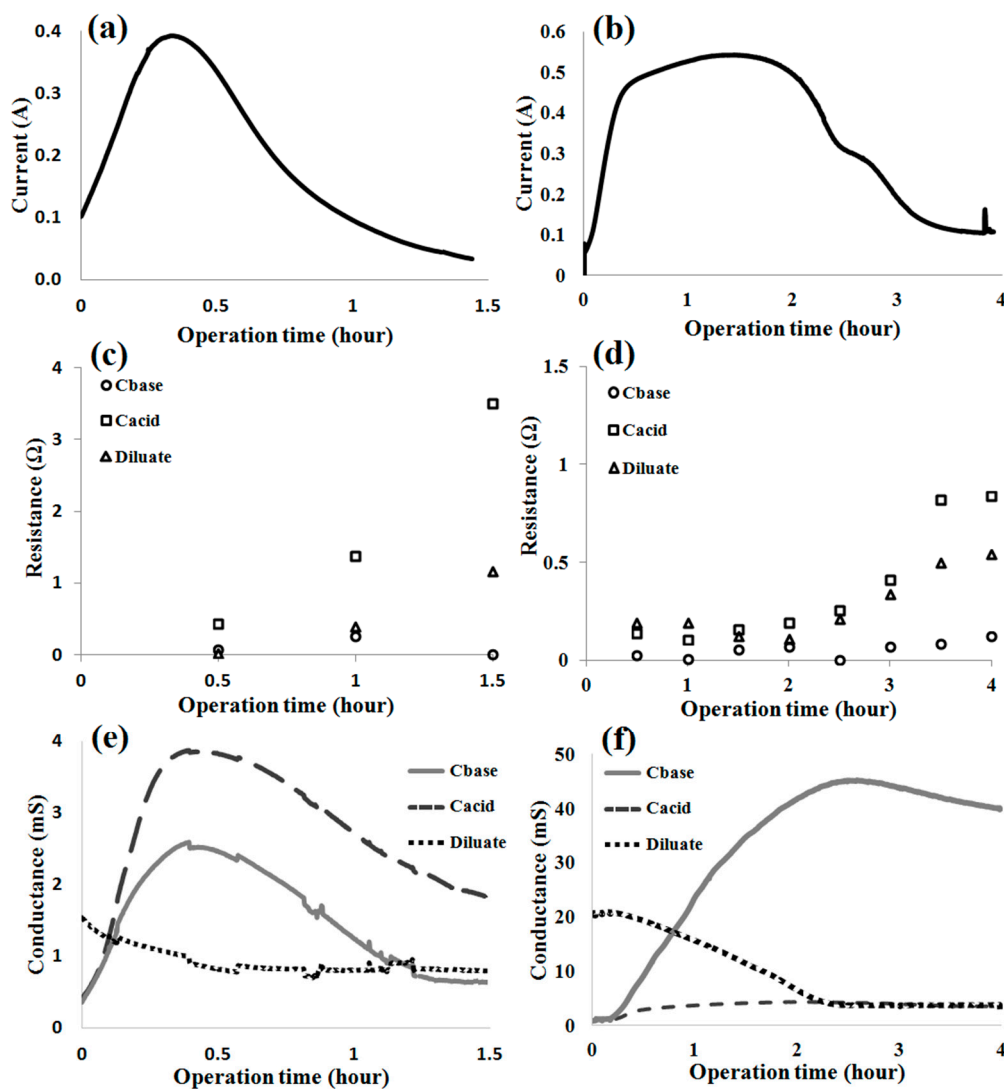


**Figure 3.** Summary of results based on the measured current (a,b), resistance calculated (c,d) and conductance of the segments (e,f). Curves (a,c,e) regarding 5 g/L IA and 15 g/L glucose content; pH = 2 and 30 V. Curves (b,d,f) regarding 33 g/L IA and 33 g/L glucose; pH = 5 and 20 V.

It can be said that using EDBM, the separation of IA from the residual glucose is conducted relatively easily since the latter component has neither ionic characteristic nor notable diffusion in this system. Nevertheless, there are other components and extracellular organic acids in the fermentation broth that have similar properties to IA, for instance, malic acid (MA), alpha-ketoglutaric acid, succinic acid, fumaric acid, etc. [27].

#### 3.4. Effects of IA Fermentation Substrate and By-Product

Compared to the previous experiments (A and B) it seemed that under lower applied potential 20V with higher initial pH 5 and higher IA concentration (around 33g/ L) could result in more efficient columbic efficiency (CE) from the viewpoint of IA separation. In the following tests, low potential (10 V) was set and the initial pH was adjusted to 3, which is an ordinary value in IA fermentation [22]. Table 3 presents the composition of the model solutions (Experiments C., D., E.) which contains: itaconic acid, glucose and malic acid. Malic acid (MA) has similar properties to itaconic acid and it is one of the main by-products generated in the course of fermentation [15].

The experiment C., where the potential was set to 10 V and the same amount of IA was separated, showed similar results (seen in Table 4) with the previous experiment (A.), where the potential was

set to 30 V. It is suggested that there is an optimal potential between 10 V and 30 V where the co-ion migration is not significant. Co-ion migration also occurred in the other cases. If the concentration was higher, the migration of co-ions would be more notable too. From the viewpoint of CE, the results indicate that the investigation with a higher IA concentration of 25–33 g/L at a low pH (2–5) could enhance the CE. To analyze MA migration, further elaboration will be needed, but the current results suggest that migration of MA was similar to IA.

In all cases, around 60–100 mL of water disappeared during the separation due to water absorption of the membrane. During the operation, the influence of water transfer mechanisms was not significant except in the case of test C., where from the diluate cycle around 100 mL of solvent moved to the  $C_{\text{acid}}$  segment. In ED or EDBM, the transport of the ions through the bulk solution and membranes is governed by the electrical potential generated between the electrodes. Water transfer (shown in Figure 1) can change the volume and the concentration of the solutions, as described by Wang [28].

There are some mechanisms that cause water transportation through the membranes. One of them is the electro-osmosis, in which transporting hydrous ions (counter-ions, co-ions) and water molecules in the solvation shell can be transported across membranes at a higher current density [32–34]. Another mechanism is hydraulic osmosis, which occurs when there is a concentration difference between diluate and the concentrate flows at a low current density [33,34]. The third water transfer mechanism is called pressure leakage, which is influenced by internal factors, such as the micropores in the membrane matrix, and external factors, such as the differential pressure between the two adjacent segments that developed due to the difference in fluid flow rates. It should be noted that this may also cause ion leakage.

Additionally, Wang et al. [28] describe some further mass transfer mechanisms during the electro dialysis process that explain some of the results in this paper—namely, hydrolytic dissociation, also known as concentration polarization [35], in which co-ion migration and the concentration diffusion of ions can also take place. The latter decreases the product concentration and the acid/alkali concentration for conventional electro dialysis (CED) and EDBM, respectively.

Based on the curves shown in Figure 4, the tendencies of the conductance (b), (d), (f) and current (a), (c), (e) data are similar to those of the previous tests (A, B). According to Fan et al., a higher bulk concentration improves conductivity but lowers permselectivity [36]. Wang et al. also highlighted that the higher initial alkali concentration causes smaller resistance and results in higher efficiency of lactic acid production [28]. In our case with different model solutions in a relatively low range of bulk concentrations (IA: 5–33 g/L; MA: 0–1.75 g/L), the conductivity improved (the resistance of the segments decreased), but the permselectivity could be preserved (PR: 90–97%). It is also supported by our previous work, where a similar system was investigated using model solutions with initial IA concentrations, initial pHs and applied potentials of 5–60 g/L, 2–8, 10–30 V, respectively. The peak CE value (up to 97 %) was achieved under the following conditions: 33 g IA/L, pH = 5 and 20 V as applied potential [21]. This means that more undesired mobile ions such as other organic ions (not only MA) in the bulk phase could decrease permselectivity. Accordingly, it appears preferable to find and maintain a relatively low level of competing ions during the continuous separation of IA from the fermentation broth.

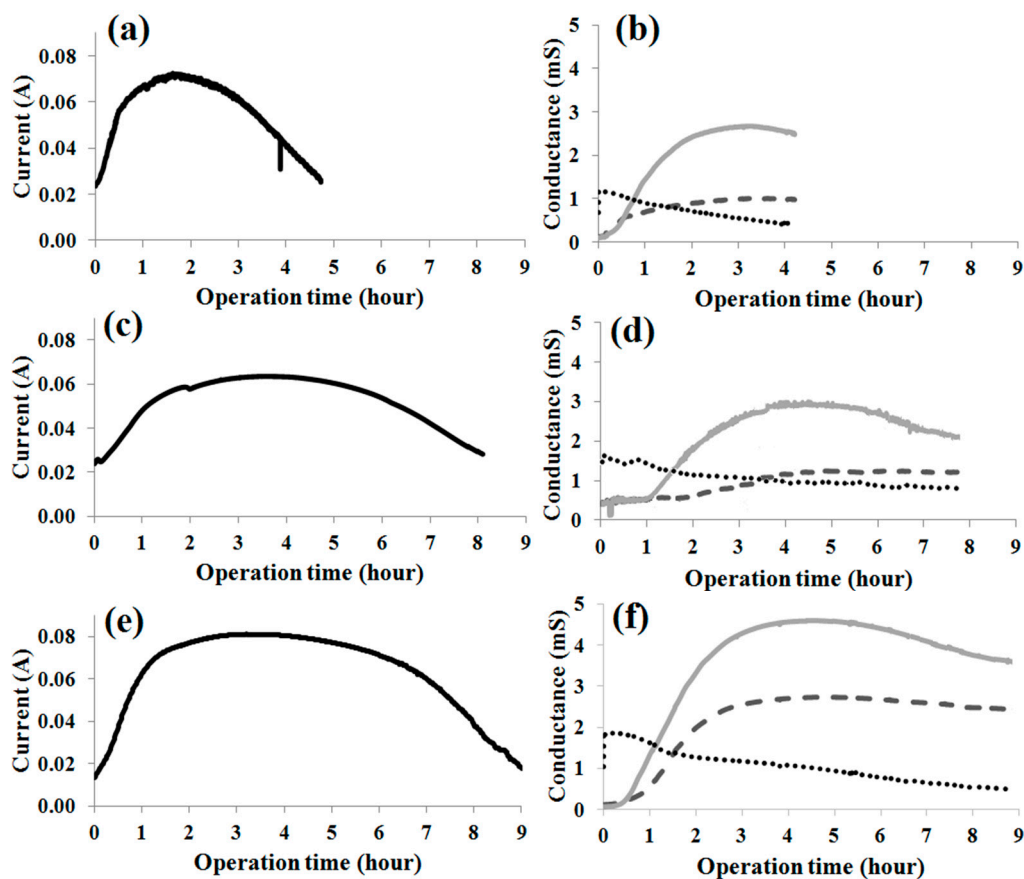


**Figure 4.** Summary of the results based on the current of the bulk in the segments (a,c,e) and the measured conductance (b,d,f). Progress curves regarding the parameters shown in Table 3, where initial pH = 3 and applied potential = 10 V in all cases. The concentration of IA: 5 g/L, 10 g/L, 15 g/L, glucose: 15 g/L, 25 g/L, 33 g/L and MA: 0.5 g/L, 0.75 g/L, 1.0 g/L were in the cases of (a) and (b), (c) and (d), (e) and (f), respectively.

#### 4. Conclusions

The steps of the classical multistep cleaning and recovery processes could be reduced with IA separation by the integrated system of fermentation and EDBM. Water dissociation by bipolar membranes is a crucial step of the separation process. The results showed that high IA recovery ratios (90–97%) and CE (74–98%) were achievable, while residual glucose did not have a negative effect on the process and could be recycled during fermentation. At the same time, due to the use of bipolar membranes, a base (NaOH) solution was generated that could be utilized, e.g., to maintain the pH of the fermentation process. In terms of CE, the initial IA concentration higher than 5 g/L was more favorable. However, the selective separation method of IA from the similarly dissolved by-products (e.g., malic acid) contained in the fermentation broth and the method of finding the optimal applied potential remain challenges. The authors intend to continue this research with a real IA fermentation mixture.

**Author Contributions:** Conceptualization, T.R., P.K., N.N.; methodology, T.R., P.K., N.N.; validation, T.R., P.K.; formal analysis, T.R., P.K.; investigation, T.R., P.K., E.K.; resources, N.N.; writing—original draft preparation, T.R., P.K., P.B.; visualization, T.R.; supervision, T.R., N.N.; project administration, N.N., K.B.-B.; funding acquisition, N.N., K.B.-B. All authors have read and agreed to the published version of the manuscript.

**Funding:** This research was supported by the National Research, Development and Innovation Fund project NKFIH OTKA K 119940 entitled “Study on the electrochemical effects of bioproduct separation by electro dialysis”.

**Conflicts of Interest:** The founding sponsors had no role in the design of the study; in the collection, analyses, or interpretation of data; in the writing of the manuscript, and in the decision to publish the results.

## References

1. Da Cruz, J.C.; De Castro, A.M.; Sérvulo, E.F.C. World Market and Biotechnological Production of Itaconic Acid. *3 Biotech* **2018**, *8*, 138. [[CrossRef](#)] [[PubMed](#)]
2. Karaffa, L.; Kubicek, C.P. *Reference Module in Life Sciences*; Elsevier: Amsterdam, The Netherlands, 2020.
3. Sriariyanun, M.; Heitz, J.H.; Yasurin, P.; Asavasanti, S.; Tantayotai, P. Itaconic Acid: A Promising and Sustainable Platform Chemical? *Appl. Sci. Eng. Prog.* **2019**, *12*, 75–82.
4. De Carvalho, J.C.; Magalhaes, A.I.; Soccol, C.R. Biobased Itaconic Acid Market and Research Trends—Is It Really a Promising Chemical? *Chim. Oggi-Chem. Today* **2018**, *36*, 56–58.
5. Anouti, F.A. Concerns Regarding Food Biotechnology: An Ongoing Debate. *J. Biodivers. Bioprospect. Dev.* **2014**, *1*, 1–3. [[CrossRef](#)]
6. Okabe, M.; Lies, D.; Kanamasa, S.; Park, E.Y. Biotechnological Production of Itaconic Acid and Its Biosynthesis in *Aspergillus Terreus*. *Appl. Microbiol. Biotechnol.* **2009**, *84*, 597–606. [[CrossRef](#)]
7. Moity, L.; Molinier, V.; Benazzouz, A.; Barone, R.; Marion, P.; Aubry, J.M. In Silico Design of Bio-based Commodity Chemicals: Application to Itaconic Acid Based Solvents. *Green Chem.* **2014**, *16*, 146–160. [[CrossRef](#)]
8. Tomić, S.L.; Mičić, M.M.; Dobić, S.N.; Filipović, J.M.; Suljovrujić, E.H. Smart Poly (2-hydroxyethyl methacrylate/itaconic acid) Hydrogels for Biomedical Application. *Radiat. Phys. Chem.* **2010**, *79*, 643–649. [[CrossRef](#)]
9. Kuenz, A.; Gallenmüller, Y.; Willke, T.; Vorlop, K.D. Microbial Production of Itaconic Acid: Developing a Stable Platform for High Product Concentrations. *Appl. Microbiol. Biotechnol.* **2012**, *96*, 1209–1216. [[CrossRef](#)]
10. Klement, T.; Büchs, J. Itaconic Acid—A Biotechnological Process in Change. *Bioresour. Technol.* **2013**, *135*, 422–431. [[CrossRef](#)]
11. Maassen, N.; Panakova, M.; Wierckx, N.; Geiser, E.; Zimmermann, M.; Bölker, M.; Blank, L.M.; Klinner, U. Influence of Carbon and Nitrogen Concentration on Itaconic Acid Production by the Smut Fungus *Ustilago Maydis*. *Eng. Life Sci.* **2014**, *14*, 129–134. [[CrossRef](#)]
12. Levinson, W.E.; Kurtzman, C.P.; Kuo, T.M. Production of Itaconic Acid by *Pseudozyma Antarctica* NRRL Y-7808 under Nitrogen-limited Growth Conditions. *Enzym. Microb. Technol.* **2006**, *39*, 824–827. [[CrossRef](#)]
13. Li, A.; Pfelzer, N.; Zuijderwijk, R.; Brickwedde, A.; Van Zeijl, C.; Punt, P. Reduced By-product Formation and Modified Oxygen Availability Improve Itaconic Acid Production in *Aspergillus Niger*. *Appl. Microbiol. Biotechnol.* **2013**, *97*, 3901–3911. [[CrossRef](#)] [[PubMed](#)]
14. Saha, B.C. Emerging Biotechnologies for Production of Itaconic Acid and its applications As a Platform Chemical. *J. Ind. Microbiol. Biotechnol.* **2017**, *44*, 303–315. [[CrossRef](#)] [[PubMed](#)]
15. Hevekerl, A.; Kuenz, A.; Vorlop, K.D. Influence of the pH on the Itaconic Acid Production with *Aspergillus Terreus*. *Appl. Microbiol. Biotechnol.* **2014**, *98*, 10005–10012. [[CrossRef](#)] [[PubMed](#)]
16. Zhang, X.X.; Ma, F.; Lee, D.J. Recovery of Itaconic acid from Supersaturated Waste Fermentation Liquor. *J. Taiwan Inst. Chem. Eng.* **2009**, *40*, 583–585. [[CrossRef](#)]
17. Komáromy, P.; Bakonyi, P.; Kucska, A.; Tóth, G.; Gubicza, L.; Bélafi-Bakó, K.; Nemestóthy, N. Optimized pH and its control strategy lead to enhanced itaconic acid fermentation by *Aspergillus terreus* on glucose substrate. *Fermentation* **2019**, *5*, 31. [[CrossRef](#)]
18. Magalhães, A.I.; De Carvalho, J.C.; Medina, J.D.C.; Soccol, C.R. Downstream Process Development in Biotechnological Itaconic Acid Manufacturing. *Appl. Microbiol. Biotechnol.* **2017**, *101*, 1–12. [[CrossRef](#)] [[PubMed](#)]
19. Varga, V.; Bélafi-Bakó, K.; Vozik, D.; Nemestóthy, N. Recovery of Itaconic Acid by Electrodialysis. *Hung. J. Ind. Chem.* **2018**, *46*, 43–46. [[CrossRef](#)]
20. Eggert, A.; Maßmann, T.; Kreyenschulte, D.; Becker, M.; Heyman, B.; Büchs, J.; Jupke, A. Integrated in-situ Product Removal Process Concept for Itaconic Acid by Reactive Extraction, pH-shift back Extraction and Purification by pH-shift Crystallization. *Sep. Purif. Technol.* **2019**, *215*, 463–472. [[CrossRef](#)]

21. Komáromy, P.; Rózsenszki, T.; Bakonyi, P.; Nemestóthy, N.; Bélafi-Bakó, K. Statistical Analysis on the Variables Affecting Itaconic Acid Separation by Bipolar Membrane Electrodialysis. *Desalin. Water Treat.* **2020**, *192*, 408–414. [[CrossRef](#)]
22. Nemestóthy, N.; Bakonyi, P.; Komáromy, P.; Bélafi-Bakó, K. Evaluating Aeration and Stirring Effects to Improve Itaconic Acid Production from Glucose Using *Aspergillus Terreus*. *Biotechnol. Lett.* **2019**, *41*, 1383–1389. [[CrossRef](#)] [[PubMed](#)]
23. Jain, A.; Jain, R.; Jain, S. *Basic Techniques in Biochemistry, Microbiology and Molecular Biology*; Humana: New York, NY, USA, 2020; pp. 181–183.
24. Tran, A.T.; Mondal, P.; Lin, J.; Meesschaert, B.; Pinoy, L.; Van der Bruggen, B. Simultaneous Regeneration of Inorganic acid and Base from a Metal Washing Step Wastewater by Bipolar Membrane Electrodialysis after Pretreatment by Crystallization in a Fluidized Pellet Reactor. *J. Memb. Sci.* **2015**, *473*, 118–127. [[CrossRef](#)]
25. Lameloise, M.L.; Lewandowski, R. Recovering l-Malic Acid from a Beverage Industry Waste Water: Experimental Study of the Conversion Stage Using Bipolar Membrane Electrodialysis. *J. Memb. Sci.* **2012**, *403*, 196–202. [[CrossRef](#)]
26. Tongwen, X.; Weihua, Y. Effect of Cell Configurations on the Performance of Citric Acid Production by a Bipolar Membrane Electrodialysis. *J. Memb. Sci.* **2002**, *203*, 145–153. [[CrossRef](#)]
27. Huang, X.; Lu, X.; Li, Y.; Li, X.; Li, J.J. Improving Itaconic Acid Production through Genetic Engineering of an Industrial *Aspergillus Terreus* Strain. *Microb. Cell Fact.* **2014**, *13*, 119. [[CrossRef](#)]
28. Wang, X.; Wang, Y.; Zhang, X.; Feng, H.; Xu, T. In-situ Combination of Fermentation and Electrodialysis with Bipolar Membranes for the Production of Lactic Acid: Continuous Operation. *Bioresour. Technol.* **2013**, *147*, 442–448. [[CrossRef](#)]
29. Tuckerman, M.E.; Marx, D.; Parrinello, M. The Nature and Transport Mechanism of Hydrated Hydroxide Ions in Aqueous Solution. *Nature* **2002**, *417*, 925–929. [[CrossRef](#)]
30. Wang, D.; Meng, W.; Lei, Y.; Li, C.; Cheng, J.; Qu, W.; Li, S. The Novel Strategy for Increasing the Efficiency and Yield of the Bipolar Membrane Electrodialysis by the Double Conjugate Salts Stress. *Polymers* **2020**, *12*, 343. [[CrossRef](#)]
31. Sun, X.; Lu, H.; Wang, J. Recovery of Citric Acid from Fermented Liquid by Bipolar Membrane Electrodialysis. *J. Clean. Prod.* **2017**, *143*, 250–256. [[CrossRef](#)]
32. Galier, S.; Roux-de Balmann, H. Study of the Mass Transfer Phenomena Involved in an Electrophoretic Membrane Contactor. *J. Memb. Sci.* **2001**, *194*, 117–133. [[CrossRef](#)]
33. Pronk, W.; Biebow, M.; Boller, M. Electrodialysis for Recovering Salts from a Urine Solution Containing Micropollutants. *Environ. Sci. Technol.* **2006**, *40*, 2414–2420. [[CrossRef](#)] [[PubMed](#)]
34. Tanaka, Y. Ion-exchange Membrane Electrodialysis for Saline Water Desalination and Its Application to Seawater Concentration. *Ind. Eng. Chem. Res.* **2011**, *50*, 7494–7503. [[CrossRef](#)]
35. Zabolotskii, V.I.; Shel'deshov, N.V.; Gnusin, N.P. Dissociation of Water Molecules in Systems with Ion-exchange Membranes. *Russ. Chem. Rev.* **1988**, *57*, 801–808. [[CrossRef](#)]
36. Fan, H.; Yip, N.Y. Elucidating Conductivity-permselectivity Tradeoffs in Electrodialysis and Reverse Electrodialysis by Structure-property Analysis of Ion-exchange Membranes. *J. Memb. Sci.* **2019**, *573*, 668–681. [[CrossRef](#)]

